

Vibrational Analysis of a Molecular Heme–Copper Assembly with a Nearly Linear Fe^{III}–CN–Cu^{II} Bridge: Insight into Cyanide Binding to Fully Oxidized Cytochrome *c* Oxidase

Matthew T. Gardner,[†] Geurt Deinum,[†] Younkyoo Kim,^{†,‡} G. T. Babcock,^{*,†} Michael J. Scott,[§] and R. H. Holm^{*,§}

Department of Chemistry and MSU LASER Laboratory, Michigan State University, East Lansing, Michigan 48824, Department of Chemistry, Hankuk University of Foreign Studies, Yongin, Kyungki-do 449-791, Korea, and Department of Chemistry, Harvard University, Cambridge, Massachusetts 02138

Received May 21, 1996[⊗]

The complete vibrational analysis of [(1-MeIm)Fe(OEP)–CN–Cu(Me₆tren)]²⁺ (**1**), which has been constructed as a model for the cyanide-ligated binuclear center in the respiratory protein cytochrome *c* oxidase, has been carried out. The resonance Raman spectra ($\lambda_{\text{exc}} = 647 \text{ nm}$) and the mid-infrared spectra display three cyanide isotope-dependent vibrational modes. Two vibrations showed monotonic decreases with increasing mass of the cyanide ligand (2182–2137–2146–2101 cm^{-1} and 535–526–526–520 cm^{-1} , respectively, for the ¹²C¹⁴N–¹³C¹⁴N–¹²C¹⁵N–¹³C¹⁵N isotopomers), and could thus be assigned to the C≡N and Fe–CN–Cu stretching vibrations, respectively. The third vibration, detected with resonance Raman, showed a zigzag-type behavior (495–487–493–485 cm^{-1} with the set of isotopomers above) with the frequency being more sensitive to ¹³C labeling of the cyanide ligand than with ¹⁵N labeling. This pattern of isotopic dependence is characteristic of a bending vibration. Additionally, with the same laser excitation frequency, the C≡N stretching mode was observed, which is the first time that this vibration has been detected in the resonance Raman spectrum of a synthetic heme–cyanide complex. The normal coordinate analysis showed marked differences between bridged and unbridged heme–cyanide complexes. Internal coordinates that are orthogonal in unbridged systems are significantly mixed in the bridged model, despite the overall linearity of the Fe–CN–Cu moiety. These measurements strengthen the proposal that cyanide bridges the two metal atoms in the cyanide-ligated, oxidized binuclear center of cytochrome *c* oxidase. A quantitative consideration of the vibrational characteristics of cyanide bound to the resting enzyme, in light of our model compound results, strongly suggests that the binuclear center is flexible and can undergo structural rearrangement to accommodate exogenous ligands. This is likely to be of mechanistic importance in both dioxygen reduction and proton translocation.

Introduction

Cytochrome *c* oxidase is the terminal electron acceptor in the respiratory electron-transfer chain of prokaryotic and eukaryotic organisms. This membrane-bound enzyme reduces molecular oxygen to water and utilizes the resultant gain in free energy to pump protons across the cell membrane.¹ The active site of this enzyme, at which oxygen is reduced to water, consists of a binuclear Cu_B/heme *a*₃ center. The recent solution of the crystal structures² of cytochrome *c* oxidase from two sources has provided new insight into the arrangement and structure of the binuclear center of the enzyme. The distance between the two metals is 4.5 Å in the resting bovine enzyme^{2a} and 5.2 Å in the bacterial system.^{2b} The close proximity of the two metals had been deduced from earlier spectroscopic, biochemical, and molecular biological studies, and a number of models have been

advanced for their function in both O₂ reduction and in the redox-coupled translocation of protons. A central issue is the extent to which the partially reduced dioxygen substrate interacts with the two metals. At the peroxide level in the reaction sequence, for example, a range of structures, from a μ -peroxy fully covalent linkage to a terminal hydroperoxy moiety (Fe–O–O–H) with minimal interaction between the Cu_B and the heme *a*₃ moiety, have been proposed.¹

Cyanide, a potent inhibitor of oxidase activity, has often been used as an alternate ligand to the heme of the binuclear center³ and can provide insight into the modes by which small molecules bind. The Soret band in the optical spectrum of heme *a*₃ shifts upon cyanide ligation as the heme iron undergoes a high-spin to low-spin transition. This shift in the optical and magnetic properties of the site has formed the basis for a variety of optical, electron paramagnetic resonance, magnetic–circular dichroism, and magnetic susceptibility studies of the CN[−] ligated enzyme.¹ A further useful spectroscopic probe is the C≡N

* To whom correspondence should be addressed.

[†] Michigan State University.

[‡] Hankuk University of Foreign Studies.

[§] Harvard University.

[⊗] Abstract published in *Advance ACS Abstracts*, October 15, 1996.

- (1) (a) Malmstrom, B. G. *Acc. Chem. Res.* **1993**, *26*, 332. (b) Babcock, G. T.; Wikstrom, M. *Nature* **1992**, *356*, 301. (c) Rich, P. R. *Aust. J. Plant Physiol.* **1995**, *22*, 479. (d) Einarsdottir, O. *Biochim. Biophys. Acta* **1995**, *1229*, 129.
- (2) (a) Tsukihara, T.; Aoyama, H.; Yamashita, E.; Tomizaki, T.; Yamaguchi, H.; Shinzawa-Itoh, K.; Nakashima, R.; Yaono, R.; Yoshikawa, S. *Science* **1995**, *269*, 1069. (b) Iwata, S.; Ostermeier, C.; Ludwig, B.; Michel, H. *Nature* **1995**, *376*, 660.

- (3) (a) Palmer, G. J. *Bioenerg. Biomembr.* **1993**, *25*, 145. (b) Caughey, W. S.; Dong, A.; Sampath, V.; Yoshikawa, S.; Zhao, X.-J. *J. Bioenerg. Biomembr.* **1993**, *25*, 81. (c) Oertling, W. A.; Surerus, K. K.; Einarsdottir, O.; Fee, J. A.; Dyer, R. B.; Woodruff, W. H. *Biochemistry* **1994**, *33*, 3128. (d) Oertling, W. A.; Kim, Y.; Babcock, G. T.; Surerus, K. K.; Fee, J. A.; Dyer, R. B.; Woodruff, W. H. *Inorg. Chem.*, in press. (e) Yoshikawa, S.; Mochizuki, M.; Zhao, X.-J.; Caughey, W. S. *J. Biol. Chem.* **1995**, *270*, 4270. (f) Yoshikawa, S.; O'Keefe, D. H.; Caughey, W. S.; *J. Biol. Chem.* **1985**, *260*, 3518.

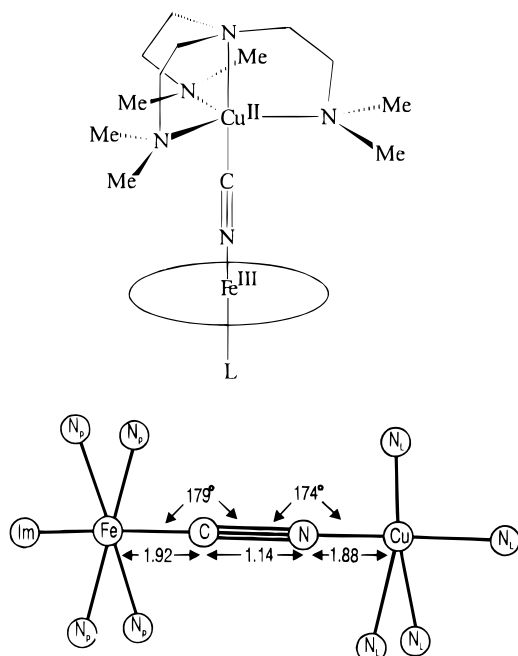


Figure 1. Top: Schematic description of the structure of $[(1\text{-MeImd})\text{-Fe}(\text{OEP})\text{-CN-Cu}(\text{Me}_6\text{tren})]^{2+}$ (OEP = octaethylporphyrinate(2-), Me_6tren = tris(*N,N*-dimethylamino)ethylamine), L = 1-methylimidazole or pyridine. Bottom: Simplified model used for normal coordinate analysis, including selected metric parameters from the corresponding complex with an axial pyridine ligand.^{4b} Circles represent the point masses used to account for ligand weights, and distances are in angstroms.

stretching vibration,⁴ which is characterized by a strong, sharp absorption around 2030–2200 cm^{-1} . This has allowed the use of infrared spectroscopy to study the interactions of bound CN^- in the binuclear center.³ Although the prevailing view of the mode of cyanide binding in the fully oxidized enzyme invokes a bridging conformation,^{3a} models have been advanced that postulate monodentate binding.^{3b} If cyanide does, in fact, bind in a bridging configuration, the vibrational behavior of the ligand, in terms of its geometry, remains to be elucidated. These are questions that can be addressed through careful vibrational spectroscopic analysis, isotopic labeling, normal coordinate analysis, and model compound studies.

A series of molecules of the general type $[(\text{N-base})\text{Fe}^{\text{III}}(\text{OEP})\text{-CN-Cu}^{\text{II}}\text{LL}']$ have been prepared as analogues of the cyanide-bound binuclear center of oxidized cytochrome *c* oxidases.⁵ Here the N-base is pyridine or 1-methylimidazole (1-MeIm), L is a tridentate or tetradentate polyamine ligand bound to four- or five-coordinate Cu(II), and L' is a unidentate anion (when present). A number of these molecular bridged assemblies have been structurally defined by crystallography. They are characterized by a six-coordinate low-spin Fe(III) atom in the mean plane of the porphyrin (≤ 0.1 Å displacement), an essentially linear Fe–C≡N group ($176\text{--}180^\circ$) of invariant bond lengths, variable Cu–N distances (1.88–2.17 Å), Cu–N–C angles ($147\text{--}174^\circ$) dependent on ligand L, and Fe–Cu separations of 4.93–5.11 Å. For this initial investigation of the vibrational properties of Fe–CN–Cu bridges, we have examined $[(1\text{-MeIm})\text{Fe}(\text{OEP})\text{-CN-Cu}(\text{Me}_6\text{tren})]^{2+}$ (**1**),^{5b} whose structure is presented schematically in Figure 1. The structure

of this complex has not been determined; metric data are from the closely related molecule with a pyridine axial ligand.^{5b} This difference in axial ligands is expected to have a negligible effect on the Fe–CN–Cu bridge parameters which, with the exception of the Cu–N bond length and the Cu–N–C angle, are essentially invariant over some six structures. The imidazole-ligated bridge assembly was chosen because of the presence of a proximal imidazole at heme a_3 in the binuclear center² and the simplifying feature of the nearly linear bridge. As in the cyanide-inhibited enzyme,⁶ the metal spins are ferromagnetically coupled in $[(\text{py})\text{Fe}(\text{OEP})\text{-CN-Cu}(\text{Me}_6\text{tren})]^{2+}$ to afford an integer spin ground state.⁷ Analogous assemblies with bridging oxo⁸ and hydroxo⁹ groups have been prepared and structurally characterized. Their magnetic properties are similar to those of the oxidized resting enzyme. These bridged assemblies, being structurally proven examples of bidentate cyanide coordination of a type possible in the enzyme, can lend insight into the structure of the binuclear center of the cyanide-inhibited protein.

In the work reported here, we have applied resonance Raman and infrared spectroscopies to **1** and varied the isotopic composition of the cyanide ligand. We then used the vibrational data to carry out a normal coordinate analysis¹⁰ of the binuclear metal/ligand core of the complex. The calculated potential energy distributions and the refined set of force constants give insight into the nature of the bonding interactions as well as possible nonbonding, or steric, constraints. The results are used to probe the details of cyanide ligation to resting cytochrome *c* oxidase.

Experimental Section

The compound $[(1\text{-MeIm})\text{Fe}(\text{OEP})\text{-CN-Cu}(\text{Me}_6\text{tren})](\text{ClO}_4)_2$ (**1**) was prepared by the reaction of equimolar $[\text{Cu}(\text{Me}_6\text{tren})(\text{CN})](\text{ClO}_4)_2$ ^{5b} (containing the desired cyanide isotopomer), $[\text{Fe}(\text{OEP})(\text{OClO}_3)]$, and 1-methylimidazole in acetone solution, followed by diffusion of several volume equivalents of ether over several days. The product separated as dark violet needles in high yield. $[(1\text{-MeIm})\text{Fe}(\text{OEP})\text{CN}]$ (**2**) was synthesized as described.^{5b} Resonance Raman spectra were obtained with solid-state samples, cooled to -80 °C in a dewar by a stream of cold dinitrogen gas. The samples were prepared by grinding the compounds with dry KBr powder and pressing to form a pellet. To obtain Raman spectra, a Coherent Kr⁺ laser (Coherent K-90) was used for excitation at 647 nm. The laser light was focused onto the sample with an incident power of 30 mW. Resonance Raman scattering was dispersed with a Spex 1877 Triplemate spectrometer and detected by a liquid-nitrogen-cooled CCD detector (EG&G OMA 4, Model 1530-CUV-1024S). Mid-infrared spectra were acquired on a Nicolet 520P FTIR spectrometer, equipped with a DTGS or liquid-nitrogen-cooled MCT-B detector or a Nicolet IR-40 FTIR spectrometer equipped with a DTGS detector. The samples were prepared as CsI pellets. Double-sided interferograms were coadded at a resolution of 2 cm^{-1} .

Results

UV–Visible Spectroscopy. The UV–vis spectrum of the title complex is characterized by a Soret absorption maximum at 403 nm, visible bands at 526 and 553 nm, and a near-

(4) Nakamoto, K. *Infrared and Raman Spectra of Inorganic and Coordination Compounds*, 4th ed.; Wiley-Interscience: New York, 1987.

(5) (a) Lee, S. C.; Scott, M. J.; Kauffmann, K.; Münck, E.; Holm, R. H. *J. Am. Chem. Soc.* **1994**, *116*, 401. (b) Scott, M. J.; Lee, S. C.; Holm, R. H. *Inorg. Chem.* **1994**, *33*, 4651. (c) Scott, M. J.; Holm, R. H. *J. Am. Chem. Soc.* **1994**, *116*, 11357.

(6) (a) Kent, T. A.; Münck, E.; Dunham, W. R.; Filter, W. F.; Findling, K. L.; Yoshida, T.; Fee, J. A. *J. Biol. Chem.* **1982**, *257*, 12489. (b) Kent, T. A.; Young, L. J.; Palmer, G.; Fee, J. A.; Münck, E. *J. Biol. Chem.* **1983**, *258*, 8543.

(7) Kauffman, K. E.; Doy, E. P.; Münck, E.; Lee, S. C.; Holm, R. H. Results to be submitted for publication.

(8) (a) Lee, S. C.; Holm, R. H. *J. Am. Chem. Soc.* **1993**, *115*, 11789. (b) Karlin, K. D.; Nanthakumar, A.; Fox, S.; Murthy, N. N.; Ravi, N.; Huynh, B. H.; Orosz, R. D.; Day, E. P. *J. Am. Chem. Soc.* **1994**, *116*, 4753.

(9) Scott, M. J.; Zhang, H. H.; Lee, S. C.; Hedman, B.; Hodgson, K. O.; Holm, R. H. *J. Am. Chem. Soc.* **1995**, *117*, 568.

(10) Wilson, E. B.; Decius, J. C.; Cross, P. C. *Molecular Vibrations*, McGraw-Hill: New York, 1955.

Table 1. Isotopic Dependence of Vibrational Frequencies^a

vibrational mode	IR/RR detected?	¹² C ¹⁴ N	¹³ C ¹⁴ N	¹² C ¹⁵ N	¹³ C ¹⁵ N
$\nu_{\text{C}\equiv\text{N}}$	IR/RR	2182	2137	2146	2101
ν	IR	535	526	526	520
δ	RR	495	487	493	485

^a Samples in solid matrix. (CsI for IR and KBr for RR. CsI facilitated concurrent measurement of far-IR region.) No isotope-dependent modes were found between 200 and 400 cm⁻¹. See individual spectra for information on specific experimental conditions.

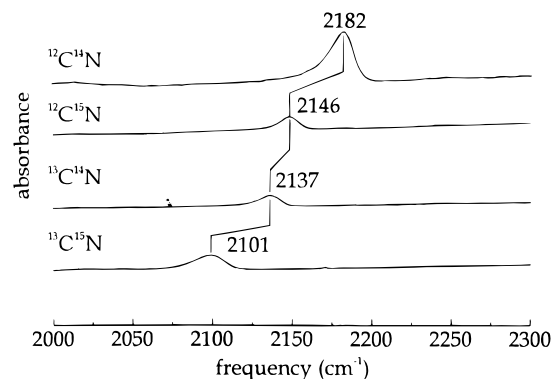


Figure 2. Mid-IR spectrum of isotopomers of [(1-MeIm)Fe(OEP)-CN-Cu(Me₆tren)]²⁺ in CsI pellet. Conditions: 128 scans, 2 cm⁻¹ resolution, DTGS detector, 25 °C. Key: (a) ¹²C¹⁴N; (b) ¹²C¹⁵N; (c) ¹³C¹⁴N; (d) ¹³C¹⁵N.

ultraviolet absorption at 345 nm. When compared to the absorption spectrum of the unbridged heme cyanide complex **2**, despite general similarity, several differences are notable. These include a small (3 nm) blueshift in the Soret maximum, a slight (3 nm) redshift of the UV absorption, and subtle band shape differences of the visible peaks.^{5b} The visible absorption bands of both the bridged binuclear complex and the unbridged heme complex show a trailing edge and small features at approximately 650 nm. These absorption bands are shown below to be important in the context of resonance Raman detection of the cyanide stretching and bending modes of this molecule.

Infrared Spectroscopy. Infrared and resonance Raman spectra of **1** display three vibrational modes that have frequencies sensitive to isotopic labeling of the cyanide moiety (Table 1). The first of these appears at 2182 cm⁻¹ in the mid-IR spectra of the molecule (Figure 2). From its frequency and relative intensity, this mode can be assigned to the C≡N stretching vibration of bound, bidentate cyanide. When the cyanide is substituted with ¹²C¹⁵N, the vibration shifts to 2146 cm⁻¹; with ¹³C¹⁴N, it shifts to 2137 cm⁻¹, and with ¹³C¹⁵N cyanide, the mode appears at 2101 cm⁻¹. This monotonic-frequency decrease with increasing mass of the ligand is expected for a C≡N stretching vibration in simple heme-cyanide complexes. The second vibrational mode that displays an isotope dependence appears in the infrared spectrum at 535 cm⁻¹ (Figure 3). With ¹³C¹⁴N or ¹²C¹⁵N, the mode appears at 526 cm⁻¹, and with the doubly labeled cyanide, the mode shifts to 520 cm⁻¹. As with the C≡N stretching mode, this absorption displays a mass-dependent decrease in frequency upon isotopic labeling and is assigned to a stretching vibration of the Fe-C≡N-Cu bridge unit.

The extinction coefficients for the C≡N stretches of **1** and **2** were determined by dissolving known amounts of the crystalline compounds in acetone. These are collected in Table 2, along with relevant extinction coefficients from related complexes.¹¹ The effect of hydrogen bonding on the $\nu_{\text{C}\equiv\text{N}}$ stretching frequency

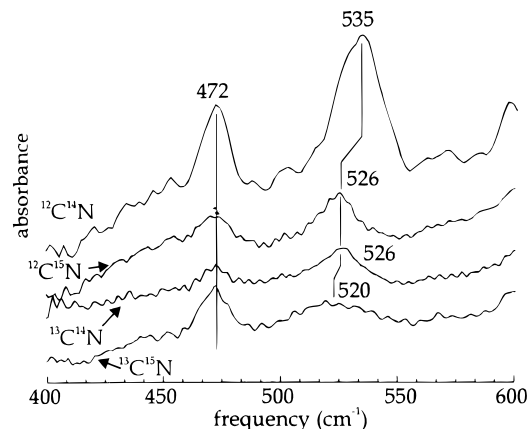


Figure 3. Mid-IR of isotopomers of [(1-MeIm)Fe(OEP)-CN-Cu(Me₆tren)]²⁺. See Figure 2 for conditions. Key: (a) ¹²C¹⁴N; (b) ¹²C¹⁵N; (c) ¹³C¹⁴N; (d) ¹³C¹⁵N.

Table 2. Extinction Coefficients of C≡N Stretches

	$\nu_{\text{C}\equiv\text{N}}$ (cm ⁻¹)	ϵ (M ⁻¹ cm ⁻¹)	ref
Fe ^{III} -C≡N	2129	17	this work
Fe ^{III} -C≡N-Cu ^{II}	2182	150	this work
Ru ^{III} -C≡N	2053	~2500	11
Ru ^{II} -C≡N-Ru ^{III}	2118	~50	11

was determined by dissolving **2** in neat methanol. A 3 cm⁻¹ shift to higher frequency was evident in methanol, indicating a distal interaction between the hydrogen bond-donating solvent, and the nitrogen atom of the cyanide ligand (see Table 3).

Resonance Raman Spectroscopy. The third cyanide isotope-sensitive vibration of **1** appears in its resonance Raman spectrum. When 647 nm excitation is used, a vibration is present at 495 cm⁻¹ in the Raman spectrum (Figure 4). In the ¹³C¹⁴N-labeled complex, this vibration shifts to 487 cm⁻¹. With ¹²C¹⁵N, the vibrational mode occurs at 493 cm⁻¹, and with doubly labeled cyanide, this mode shifts to 485 cm⁻¹. This type of zigzag isotopic dependence is diagnostic of a bending vibration of the Fe-C≡N unit. The observation of heme-ligated cyanide and heme-ligated CO bending modes in enzymatic systems is well preceded in the literature;^{1,12} however, this vibration has not previously been observed in synthetic porphyrin systems.¹³

When higher-frequency Raman scattering was examined with 647 nm excitation, an isotope-sensitive mode was observed at 2182 cm⁻¹ (Figure 5). Upon isotopic substitution, the shifts correlated with those observed in the infrared spectrum for the C≡N stretching mode, allowing its assignment as the normally infrared active/Raman inactive C≡N stretching mode. Resonance Raman detection of the C≡N stretching mode has no precedent in cyanide-ligated heme systems.

Vibrational Analysis. Normal coordinate analysis (NCA) was performed to assign the vibrational modes of **1** and to determine the contributions of individual internal coordinates to the vibrational modes of the complex. The model used to represent **1** is shown in Figure 1. The heme was represented by four point masses, arranged equatorially around a six-coordinate iron atom. The four non-cyano ligands to the five-

- (11) Doorn, S. K.; Dyer, R. B.; Stoutland, P. O.; Woodruff, W. H. *J. Am. Chem. Soc.* **1993**, *115*, 6398.
- (12) (a) Lopez-Garriga, J. L.; Oertling, W. A.; Kean, R. T.; Hoogland, H.; Wever, R.; Babcock, G. T. *Biochemistry* **1990**, *29*, 9387. (b) Yu, N.-T.; Benko, B.; Kerr, E. A.; Gersonde, K. *Proc. Natl. Acad. Sci. U.S.A.* **1984**, *81*, 5106.
- (13) (a) Uno, T.; Hatano, K.; Nishimura, Y.; Arata, Y. *Inorg. Chem.* **1988**, *27*, 3215. (b) Kerr, E. A.; Mackin, H. C.; Yu, N.-T. *Biochemistry* **1983**, *22*, 4373.

Table 3. Vibrational Frequencies for C≡N in Selected Structures

CN geometry/N-terminus interaction	example	ranges of ν_{CN} (cm^{-1})	ref
linear/none	[(1-MeIm)Fe(OEP)(CN)]	2129	this work
bent/none	SP-14 ("strapped-heme")	2118–2130	16
linear/hydrogen-bonded	oxidized HRP, 2 in methanol	2131, 2132	12, this work
bent/hydrogen-bonded	no published examples		
linear/Cu-bonded	1 , Fe–CN–Cu	2140–2182	5, this work
bent/Cu-bonded	Fe–CN–Cu ($\theta < 140$ – 170°) ^a	2120–2181	5, this work
	oxidized cytochrome <i>c</i> oxidase	2146–2152	3

^a θ = angle defined by Cu–N≡C.

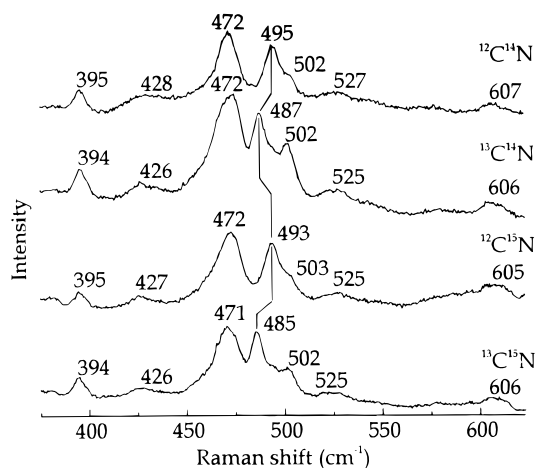


Figure 4. Resonance Raman of isotopomers of [(1-MeIm)Fe(OEP)–CN–Cu(Me₆tren)]²⁺. See Experimental Section for details. Key: (a) ¹²C¹⁴N; (b) ¹³C¹⁴N; (c) ¹²C¹⁵N; (d) ¹³C¹⁵N.

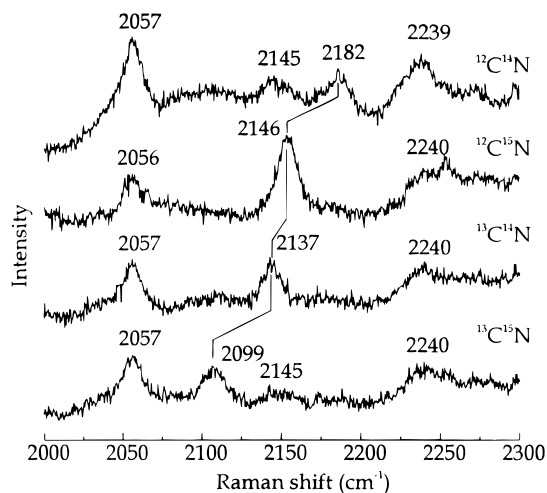


Figure 5. Resonance Raman of isotopomers of [(1-MeIm)Fe(OEP)–CN–Cu(Me₆tren)]²⁺. See Experimental Section for details. Key: (a) ¹²C¹⁴N; (b) ¹²C¹⁵N; (c) ¹³C¹⁴N; (d) ¹³C¹⁵N.

coordinate copper atom were treated as point masses, with each weighing one-fourth of the total ligand mass. The 1-methylimidazole was also approximated by a point mass representing the total weight of the ligand.

The NCA was performed to find the best set of force constants that duplicated the observed cyanide isotopic shifts of the vibrational frequencies in **1** (Table 1). The frequencies used to fit the data were the infrared observed modes at 2182 and 535 cm^{-1} and the observed Raman peak at 495 cm^{-1} . The optimized force field for this molecule is listed in Table 4. The experimental and calculated vibrational frequencies for the cyanide isotope-sensitive modes, along with the potential energy distributions for these modes, are collected in Table 5.

The potential energy distribution (PED) for the 2182 cm^{-1} band (Table 5) shows that this mode is comprised entirely of the C≡N stretching coordinate. The shifts observed are duplicated by a simple, two-body harmonic oscillator, further supporting the potential energy distribution calculated in the complete analysis. An interesting result is found for the potential energy distribution of the 535 cm^{-1} peak. This mode is comprised of roughly equal contributions of the Fe–C (35%) and Cu–N (30%) stretching coordinates, with smaller contributions from the Fe–C_N≡N_{CN} bending mode (16%). Earlier results^{12,13} indicate that, when ligands are bound to hemes in a linear geometry, the stretching and bending modes are orthogonal to each other, with each mode contributing little to the PED of the other. For **1**, however, despite the linear geometry, a substantial contribution of the stretching coordinates to the bending modes was observed; conversely, the bends contribute significantly to the predominantly stretching modes. The interaction force constant for coupling between the Fe–C stretch and the Cu–N stretch has a value of -0.19 $\text{mdyn}/\text{\AA}$ (Table 4). The PED for the 495 cm^{-1} peak (Table 5) shows that this mode is comprised of the Fe–C≡N bending coordinate, (68%), the Fe–C stretch (18%) and the Cu–N≡C (13%) bending mode. As in the case of the 535 cm^{-1} peak, there is an appreciable contribution of the stretching coordinate to what is, overall, a bending vibration. A series of control calculations demonstrated that substantially varying the Cu/non-cyanide ligand or the Fe/porphyrin force constants did not have a large effect on either the frequency or the potential energy distribution of the isotope-sensitive vibrational modes.

Discussion

Electronic Structure and Vibrational Characteristics. The vibrational properties of **1** were investigated with the use of isotopically labeled cyanide. To understand the bonding nature of cyanide, one must have a clear picture of the electronic structure of this ligand. When cyanide is bound to a metal porphyrin system, the cyanide ligand binds preferentially via the carbon end and acts as a σ -donor, lowering the electron density in its $5\sigma^*$ highest-occupied molecular orbital, which is antibonding.^{14a} This enables more efficient C≡N bonding. Consequently, a terminally bound cyanide moiety generally has a higher C≡N stretching frequency than does free cyanide. This is in contrast to the isoelectronic example of carbon monoxide, which acts preferentially as a π -acceptor and is a poor σ -donor. When terminally bound, it readily accepts electron density into its $2p\pi^*$ orbital, which lowers the C=O vibrational frequency relative to free CO.

When cyanide acts as a bidentate ligand, forming units of the type M–C≡N–M', $\nu_{\text{C}\equiv\text{N}}$ will further increase, and the metal–ligand stretching frequency will decrease.¹⁴ This can

(14) (a) Sano, M; Yamatera, H. *Chem. Phys. Lett.* **1979**, *60*, 257. (b) Dows, D. A.; Haim, A.; Wilmarth, W. K. *J. Inorg. Nucl. Chem.* **1961**, *22*, 33. (c) Alvarez, S.; Lopez, C.; Bermejo, M. J. *Transition Met. Chem.* **1984**, *9*, 123.

Table 4. Force Constants

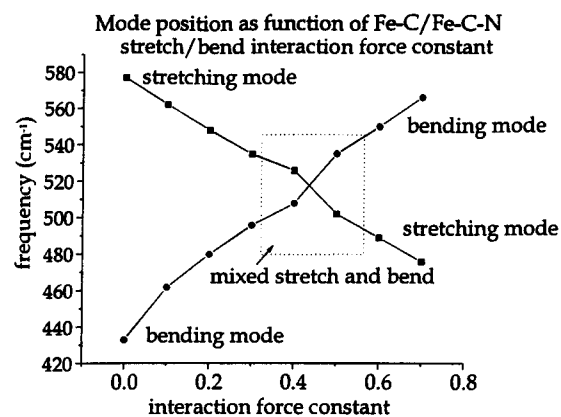
Primary			
stretches	value (mdyn/Å)	stretches	value (mdyn/Å)
Fe–C _{CN}	1.69	N _{CN} –Cu	1.26
C _{CN} –N _{CN}	17.91	Fe–N _{porph}	1.4
imd–Fe	1.55	Cu–N _{ligand}	1.0
bends	value ((mdyn Å)/rad ²)	bends	value ((mdyn Å)/rad ²)
Fe–C _{CN} –N _{CN}	0.705	out-plane imd–Fe–C _{CN}	0.2
Cu–N _{CN} –C _{CN}	0.19	in-plane Cu–N _{CN} –C _{CN}	0.2
in-plane imd–Fe–C _{CN}	0.2	out-plane Cu–N _{CN} –C _{CN}	0.2
Off-Diagonal			
stretch–stretch	value (mdyn/Å)	stretch–stretch	value (mdyn/Å)
Fe–C _{CN} /C _{CN} –N _{CN}	0.35	Cu–N _{CN} /C _{CN} –N _{CN}	0.1
Fe–C _{CN} /Cu–N _{CN}	–0.19	C _{CN} –N _{CN} /imd–Fe	0.09
Fe–C _{CN} /imd–Fe	0.1	Cu–N _{CN} /Cu–L _{ax}	0.1
stretch–bend	value (mdyn/rad)	stretch–bend	value (mdyn/rad)
Fe–C _{CN} /Fe–C _{CN} –N _{CN}	0.3	Cu–N _{CN} /Fe–C _{CN} –N _{CN}	0.07
Fe–C _{CN} /Cu–N _{CN} –C _{CN}	–0.17	Cu–N _{CN} /Cu–N _{CN} –C _{CN}	–0.55
bend/bend		value ((mdyn Å)/rad ²)	
Fe–C _{CN} –N _{CN} /Cu–N _{CN} –C _{CN}		0.17	

Table 5. Experimental and Calculated Vibrational Frequencies (cm^{–1})

¹² C ¹⁴ N		¹² C ¹⁵ N		¹³ C ¹⁴ N		¹³ C ¹⁵ N		potential energy distribution
exptl	calcd	exptl	calcd	exptl	calcd	exptl	calcd	
2182	2182	2146	2148	2137	2136	2101	2102	99% C _{CN} –N _{CN} stretch
535	535	526	527	526	527	520	519	35% Fe–C _{CN} stretch, 30% N _{CN} –Cu stretch, 19% Fe–C _{CN} –N _{CN} bend
495	496	493	492	487	487	485	483	68% Fe–C _{CN} –N _{CN} bend, 18% Fe–C _{CN} stretch, 13% Cu–N _{CN} –C _{CN} bend

be rationalized with simple molecular orbital arguments. Introducing a bonding interaction at the nitrogen atom of the bound cyanide will deplete electron density in the molecular orbital carrying the electron density at that end of the molecule. This orbital is an overall σ^* antibonding orbital, and depleting electron density leads to a higher overall C \equiv N stretching force constant. Another prediction made by the molecular orbital argument is that the M–CN bond will be weaker in a bridging geometry. However, in the case of the bridged system presented here, the vibration attributed to the metal–cyanide stretching mode appears at a significantly *higher* frequency, 535 cm^{–1}, than that of the corresponding unbridged system, **2**, whose Fe–CN vibration appears at 450 cm^{–1}.¹³ This observation can be rationalized by examining the force constants and the resulting PED of the normal coordinate analysis (Tables 4 and 5). It is seen that the force constant for the Fe–C stretch is indeed lower (1.69 mdyn/Å) than that found in studies of the corresponding unbridged system (\sim 2.01 mdyn/Å),¹³ indicating a weaker interaction between the iron and the carbon end of the cyanide ligand in the bridged as compared to the unbridged systems. The basis for this paradoxical behavior, i.e. an observed increase in stretching frequency despite a lower stretching force constant, is discussed in the following section.

Normal Mode Composition. Previous studies have undertaken careful analyses of the normal mode compositions of the vibrational frequencies of heme/cyanide complexes. These studies have identified characteristic interdependencies for certain bending and stretching vibrations. For example, there is little or no interaction between the Fe–C \equiv N bending mode and the orthogonal Fe–C stretching internal coordinate in systems in which the ligand binding is parallel to the normal of the heme plane. An example of this is cyanoferric horseradish peroxidase^{12a} in which the cyanide binds linearly. For this complex, the stretch/bend (S/B) interaction force constant is small, 0.079 mdyn/rad. In **1**, however, in which the ligand binds

**Figure 6.** Plot of the calculated frequencies for the bending and stretching mode position as a function of the Fe–C stretch/Fe–C \equiv N bending interaction force constant.

in an analogous, almost linear, fashion (179° Fe–C \equiv N angle), an appreciable interaction force constant (IFC) of 0.3 mdyn/rad between these two coordinates is necessary to maintain the relative ordering of the bending and stretching modes. The effect of changing the value of this interaction force constant on the relative ordering of the bending and stretching vibrations is shown in Figure 6. At vanishing values of this interaction force constant, the stretching mode is higher in frequency than the bending mode. As the IFC value is increased, the bending and stretching modes approach each other, then cross at a value of \sim 0.42 mdyn/rad. At values for the IFC above 0.42 mdyn/rad the bending mode is predicted to be higher in frequency than the stretching mode. The value that best reproduces the observed bending and stretching bands at 495 and 535 cm^{–1}, respectively, is 0.30 mdyn/rad. The value of the interaction force constant also affects the mode composition of the two normal modes. Values for the IFC of approximately 0.3–0.6 mdyn/rad increase the amount of mixing of the Fe–C \equiv N

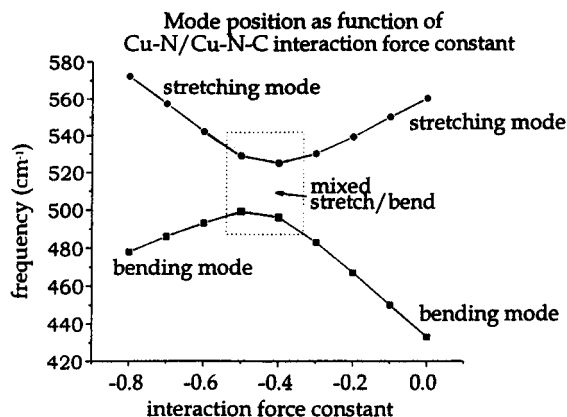


Figure 7. Plot of the calculated frequencies for the bending and stretching mode position as a function of the Cu–N stretch/Cu–N≡C bending interaction force constant.

bending coordinate with the Fe–C stretching coordinate. At values near the point where the ordering of the bending and stretching modes switch (0.42 mdyn/rad), this mixing eliminates the characteristic zigzag isotope dependence of either band.

When the bending and stretching mode compositions and frequencies were examined as a function of the Cu–N/Cu–N≡C stretch/bend IFC, similar behavior at the limits of the range examined was observed (Figure 7). However, instead of the modes switching their ordering around a specific value for the IFC, they veer away, maintaining the stretching mode at a higher frequency than the bending mode. There are two possible values for this IFC, -0.55 mdyn/rad and -0.30 mdyn/rad, that give the observed frequency difference between the bending and stretching modes. Only with the more negative value of -0.55 mdyn/rad, however, did the absolute frequencies for the two modes match the experimentally observed frequencies.

In cyanoferric myeloperoxidase,^{12a} the ordering of the ν_1 stretching and the bending coordinates is strongly dependent upon the choice of the Fe–C stretching force constant. Additionally, the relative splitting of these modes was found to correlate with the relative linearity of the ligand. In **1**, the Fe–C≡N angle is approximately 179° .^{5b} According to the trends discussed in previous work,¹² this linear geometry would produce a stretching frequency higher than that of the bend, which is, in fact what is observed here for **1**. The higher stretching frequency is not due to an increased stretching force constant, but rather to a coupling of two stretches, where the two individual force constants are lower than those in unbridged complexes. In a study of reduced cytochrome *c* oxidase^{3d} the authors argued against cyanide bridging the iron atom of heme a_3 and Cu_B primarily on the grounds that simply introducing a Cu–N force constant into an otherwise static forcefield eliminates the characteristic zigzag isotope dependence of the bending vibration. We show here that a bridged structure, which necessitates a Cu–N force constant, can be present and that the bending mode still exhibits the expected zigzag isotope dependence characteristics. In other words, the bridging nature of cyanide in this molecule does not preclude it from exhibiting isotope-dependent shifts generally associated with a bending motion.

Resonance-Enhancement Conditions. In this work, the normally infrared active C≡N stretching vibration is observed in the resonance Raman spectrum of this complex when $\lambda_{\text{ex}} = 647$ nm. Measurements made with laser excitation in resonance with the π, π^* transitions did not exhibit any cyanide isotope-dependent modes. In carbon monoxide bound systems, distal steric constraints have been shown to influence the Raman/IR

activity of the C≡O stretch.¹⁵ The fact that the C≡N vibration is observed with red excitation indicates the presence of an absorption band with charge transfer character in the red region of the electronic absorption spectrum. The failure to observe $\nu_{\text{C}\equiv\text{N}}$ in the red excitation Raman spectrum of **2** indicates that an analogous CT band is apparently not present in this wavelength range in the absorption spectrum of the unbridged complex. This suggests that copper in the model complex and, by implication, Cu_B in the heme/copper terminal oxidases plays a significant role in defining the electronic structure of the binuclear center.

Relevance to Cytochrome *c* Oxidase. The question remains as to whether cyanide covalently bridges the two metals of the binuclear center in cyanide-treated, fully-oxidized terminal oxidases. An alternative possibility has been raised by Caughey and co-workers^{3e} that invokes a strong hydrogen-bonding interaction between the N-terminus of the cyanide ligand and a neighboring amino acid residue in the distal pocket. These models are based partly upon the $\nu_{\text{C}\equiv\text{N}}$ of $2146\text{--}2151$ cm^{-1} observed in the cyanide-inhibited enzyme.³ This and other lines of evidence need to be considered when evaluating these possibilities.

Cyanide, when not subject to steric or electronic perturbations, prefers to bind to ferric hemes in a linear fashion. An example of this situation is **2**. The $\nu_{\text{C}\equiv\text{N}}$ frequency exhibited by this linear system is 2129 cm^{-1} . When the cyanide ligand is forced, by virtue of steric or electronic constraints, to adopt a non-linear binding geometry, the $\nu_{\text{C}\equiv\text{N}}$ is correspondingly lower, as seen in the hindered, strapped heme system developed by Chang *et al.*¹⁶ The $\nu_{\text{C}\equiv\text{N}}$ for these systems ranges from 2130 cm^{-1} for a linear binding geometry, to 2118 cm^{-1} for a CN ligand with a Fe–C≡N binding angle of 130° (Table 3). The trend is that linear cyanide groups have higher C≡N stretching frequencies than those exhibited by non-linear systems. When the terminal nitrogen of a linear cyanide group is allowed to interact with an electron acceptor, $\nu_{\text{C}\equiv\text{N}}$ increases. For example, in oxidized horseradish peroxidase, in which groups capable of donating hydrogen bonds are present in the ligand binding pocket, $\nu_{\text{C}\equiv\text{N}}$ occurs at 2131 cm^{-1} (Table 3). When **2** is dissolved in methanol, a hydrogen bond donor, the $\nu_{\text{C}\equiv\text{N}}$ shows a small (3 cm^{-1}), but discernible, upshift in value (Table 3). This shift is attributed to a hydrogen bonding interaction between the solvent and the N-terminal end of the CN ligand. In complexes that are both nonlinear *and* have the N-terminus interacting with an electron acceptor (such as a hydrogen bond donor or a copper ion), a range of $\nu_{\text{C}\equiv\text{N}}$ values is displayed. These frequencies are convolutions of both the specific binding angle and the N-terminus interaction.

As shown in Table 3, the only systems whose $\nu_{\text{C}\equiv\text{N}}$ values bracket that observed in cyanide-treated cytochrome *c* oxidase are those with a copper(II) ion coordinated to the N-terminus of the cyanide ligand. These models are characterized by a relatively linear Fe–C≡N geometry, and varying angles at which the Cu(II) ion is coordinated to the N-terminus of the cyanide ligand. The model complex studied here presents one example of essentially linear (176°) Fe–C≡N and C≡N–Cu (174°) binding angles. The $\nu_{\text{C}\equiv\text{N}}$ observed in this case is 2182 cm^{-1} . Clearly, the observed value of $\nu_{\text{C}\equiv\text{N}}$ in cyanide-treated cytochrome oxidase necessitates invoking more than a simple distal hydrogen bond *and* a relatively linear binding geometry to rationalize the relatively high observed frequency for this vibration in the enzyme. We conclude that the vibrational

(15) Spiro, T. G. *Biological Applications of Resonance Raman Spectroscopy*; Spiro, T. G., Ed.; Wiley: New York, 1988; Vol. 3.

(16) Tanaka, T.; Yu, N. -T.; Chang, C. K. *Biophys J.* **1987**, *52*, 801.

analysis presented here provides strong evidence for a bridging structure in the cyanide complex of oxidized cytochrome oxidase.

It has been suggested that the intensity of the $\text{C}\equiv\text{N}$ stretch in bridging complexes is significantly lower than the $\text{C}\equiv\text{N}$ stretch in unbridged systems.^{3e} Because of this apparent trend, it was argued that the $\text{C}\equiv\text{N}$ stretching bands observed in cytochrome *c* oxidase were far too intense to arise from a bridging geometry. However, this argument is weakened by the fact that the authors based their conclusions on studies that were narrow in scope and of questionable relevance. Table 2 presents the extinction coefficients of the $\text{C}\equiv\text{N}$ stretch of some previously reported complexes¹¹ and **1** and **2** in acetone solutions. It can be seen for the ruthenium systems that the bridged cyanide exhibits a much lower extinction coefficient than does the corresponding unbridged system. However, in the case of the models studied here, the extinction coefficient of the $\text{C}\equiv\text{N}$ stretch is significantly higher in the bridged case, relative to the unbridged case. Therefore, arguments for or against the bridging of cyanide in cytochrome oxidase based upon the intensity of the cyanide stretching vibrations are not well founded.

An interesting feature of the binuclear center in the bovine resting enzyme that has emerged in the crystal structure^{2a} is that Cu_B is positioned 1 Å off the normal of the heme a_3 plane. From simple geometric arguments (assuming reasonable distances for the Fe—C and $\text{C}\equiv\text{N}$ distances and the 4.5 Å distance

provided by the crystal structure to accommodate a linear Fe—C≡N angle), the $\text{C}\equiv\text{N}$ —Cu bond angle would be 138°. From the correlation published by Scott and Holm,^{5c} this would lead to a Cu—N distance of ≈ 2.4 Å and $\nu_{\text{C}\equiv\text{N}} \approx 2120$ cm^{-1} . However, the $\nu_{\text{C}\equiv\text{N}}$ observed for cyanoferric cytochrome *c* oxidase is 2151 cm^{-1} .^{3e} This frequency correlates with a Cu—N distance of ≈ 2.1 Å and a Cu—N≡C angle ≈ 155 – 160° . This implies that the Cu_B ion must be displaced from the position seen in the crystal structure of the oxidized bovine enzyme,^{2a} which would require a certain degree of structural flexibility in the protein structure near the binuclear center of cytochrome *c* oxidase. Indeed, this is supported by the observation of a Fe—Cu distance of 5.2 Å in the azide-treated bacterial oxidase.^{2b} Electron density is detected between the two metals of the binuclear center, due either to the presence of a ligated solvent or azide molecule, while no intermetal electron density is detected in the resting, oxidized bovine system. This variable Fe—Cu distance indicates that the binuclear center has the ability to alter its geometry to accommodate exogenous ligand binding.

Acknowledgment. M.T.G., G.D., and G.T.B. acknowledge the National Institutes of Health (Grant GM-25480) for financial support and Dr. Einhard Schmidt for providing preliminary data. Research at Harvard University was supported by the National Science Foundation (Grants CHE 92-0387 and 94-3830).

IC960575Q